Pharm Res (2013) 30:847–856
DOI 10.1007/s11095-012-0926-y

RESEARCH PAPER

Involvement of a Novel Organic Cation Transporter in Verapamil Transport Across the Inner Blood-Retinal Barrier

Yoshiyuki Kubo • Yusuke Kusagawa • Masanori Tachikawa • Shin-ichi Akanuma • Ken-ichi Hosoya

Received: 26 June 2012 / Accepted: 5 November 2012 / Published online: 22 November 2012

ABSTRACT

Purpose To clarify the transport and inhibition characteristics involved in verapamil transport across the inner blood-retinal barrier (inner BRB).

Methods The transport of [^{3}H]verapamil across the inner BRB was investigated using retinal uptake index and integration plot analyses in rats. The detailed transport characteristics were studied using TR-iBRB2 cells, a conditionally immortalized rat retinal capillary endothelial cell line that is an *in vitro* model of the inner BRB.

Results The apparent influx permeability clearance of [^{3}H]verapamil was 614 μL/(min·g retina), which is 4.7-fold greater than that of brain. The retinal uptake of [^{3}H]verapamil was slightly increased by 3 mM verapamil and 10 mM qunidine and inhibited by 40 mM pyrilamine, supporting the carrier-mediated efflux and influx transport of verapamil across the inner BRB. TR-iBRB2 cells exhibited a concentration-dependent uptake of [^{3}H]verapamil with a K_m of 61.9 μM, and the uptake was inhibited by several cations, such as pyrilamine, exhibiting a different profile from the identified transporters. These transport properties suggest that verapamil transport at the inner BRB takes place *via* a novel organic cation transporter.

Conclusions Our findings suggest that a novel organic cation transporter is involved in verapamil transport from the blood to the retina across the inner BRB.

KEY WORDS inner blood-retinal barrier · lipophilic basic drug · organic cation transporter · P-glycoprotein

INTRODUCTION

The blood-retinal barrier (BRB) is located between the retinal tissue and the circulating blood, and it is known that the responsible cells at the BRB are retinal pigment epithelial (RPE) cells and retinal capillary endothelial cells, forming the outer and inner BRB, respectively (1–3). Although the inner BRB prevents passive diffusion *via* paracellular solute transport, the inner BRB efficiently provides the retina with essential nutrients from the circulating blood (3).

In retinal capillary endothelial cells, the expression of various transporters has been reported including transporters for low-molecular weight molecules, such as D-glucose (4), monocarboxylates (5), amino acids (6), organic cations and vitamins (7,8), at the inner BRB. These contribute to the transport of nutrients to the retina from the circulating blood and the involvement of transporters, such as L (leucine-referring) amino acid transporter 1 (LAT1/Slc7a5) and monocarboxylate transporter 1 (MCT1/Slc16a1), in drug transport across the BRB has been reported (5,6). Organic anion transporting polypeptide 1a4 (oatp1a4/oatp2/Slco1a4), organic anion transporter 3 (Oat3/Slc22a8) and multidrug resistance protein 4 (Mrp4/Abcc4) are involved in the efflux transport of endogenous metabolites, such as estradiol 17-β-D-gluconide and dehydroepiandrosterone sulfate, and anionic drugs including benzylpenicillin, 6-mercaptopurine, and *p*-aminohippuric acid (PAH) across the inner BRB (3,9–11). In addition, P-glycoprotein (P-gp/Mdr1/Abcb1) is localized in the luminal membrane of retinal capillary endothelial cells to restrict the distribution of lipophilic and cationic drugs to the neural retina (12,13). Therefore, it is not easy to achieve systemic drug delivery to the retina which is important because retinal diseases, such as diabetic retinopathy, are in major therapeutic targets.

Electronic supplementary material The online version of this article (doi:10.1007/s11095-012-0926-y) contains supplementary material, which is available to authorized users.

Y. Kubo · Y. Kusagawa · M. Tachikawa · S. Akanuma · K. Hosoya (✉)
Department of Pharmaceutics
Graduate School of Medicine and Pharmaceutical Sciences
University of Toyama
2630, Sugitani
Toyama 930-0194, Japan
e-mail: hosoyak@pha.u-toyama.ac.jp

M. Tachikawa
Division of Membrane Transport and Drug Targeting
Graduate School of Pharmaceutical Sciences, Tohoku University
Sendai, Japan

In BRB research, information about *in vivo*/*in vitro* relationships is helpful for predicting drug distribution to the retina, and Kadam and Kompella and Toda *et al.* have reported lipophilicity-based estimations of *in vivo* drug distribution to ocular tissue (14,15). Previously, we also reported a close correlation between the lipophilicity (log *DC* value; log *n*-octanol/Ringer distribution coefficient) and the retinal uptake index (RUI) for a variety of chemical classes, using 13 compounds that were expected to undergo blood-to-retina-directed passive diffusion and had log *DC* values ranging from −2.6 to 2.5 (16). Although a predictable relationship between the RUI and log *DC* values was shown for compounds that display no significant influx and efflux transport, substantially higher RUI values than those of our lipophilicity-based prediction were exhibited by several compounds, such as D-glucose, L-arginine, L-leucine, and L-Dopa, which are substrates of influx transporters (16).

In contrast, the substrates of P-gp exhibited interesting results, and verapamil had a 5.3-fold greater RUI value than that of the lipophilicity trend line in spite of the lower RUI values shown by digoxin and vincristine (16–19), suggesting the possible involvement of carrier-mediated influx transport process(es) in verapamil transport across the BRB. However, our knowledge of the verapamil transport at the inner BRB was incomplete and there was a report that an unknown cation transporter contributes to verapamil transport at the outer BRB (20). Verapamil, a cationic Ca^{2+} channel blocker, is a drug used for the treatment of arterial hypertension and arrhythmia (21), and it has been also studied as an anti-glaucoma drug (22). Therefore, in order to achieve systemic drug delivery to the retina, more detailed evidence about the transport of verapamil at the inner BRB will be helpful.

The purpose of this study is to clarify the properties of verapamil transport across the inner BRB, such as the involvement of carrier-mediated transport, the inhibitory profile and molecules which might be candidate transporters. The mechanisms governing verapamil influx transport at the inner BRB were investigated by *in vivo* vascular injection methods and an uptake study using TR-iBRB2 cells. TR-iBRB2 cells are a key *in vitro* tool to study the inner BRB since they have similar cell morphology and gene expression profile to retinal capillary endothelial cells, and are significantly correlated with *in vivo* BRB permeability (23–25).

MATERIALS AND METHODS

Animals

The experimental protocols for the present animal study conformed to the provisions of the ARVO (The Association for Research in Vision and Ophthalmology) Statement and were approved by the Animal Care Committee, University of Toyama. Male Wistar rats (160–180 g) were purchased from Japan SLC (Hamamatsu, Japan) and kept in a controlled environment.

Reagents

[N-methyl-^{3}H]Verapamil hydrochloride ([^{3}H]verapamil, 80 Ci/mmol) and *n*-[1-^{14}C]butanol ([^{14}C]*n*-butanol, 2 mCi/mmol) were purchased from American Radiolabeled Chemicals (St. Louis, MO). [Pyridinyl-5-^{3}H]pyrilamine ([^{3}H]pyrilamine, 20 Ci/mmol) was purchased from PerkinElmer Life and Analytical Sciences (Waltham, MA). Nipradilol was kindly provided by Kowa Co., Ltd. (Nagoya, Japan). All other chemicals were of reagent grade and available commercially.

Blood-to-Retina [^{3}H]Verapamil Transport Study

Integration plot analysis was performed as described previously (8,26,27). In order to determine the apparent influx permeability clearance (K_{in}) of [^{3}H]verapamil in the retina, [^{3}H]verapamil (3 μCi/rat) in 400 μL (93.8 nM) Ringer-HEPES buffer (141 mM NaCl, 4 mM KCl, 2.8 mM $CaCl_2$, 10 mM HEPES, pH 7.4) was injected into the femoral vein of rats anesthetized with pentobarbital (50 mg/kg body weight).

The retinal and brain uptake index (RUI and BUI) methods were carried out as described previously (8,16,28,29). To evaluate the inhibitory effects of cationic compounds (3–40 mM) on the blood-to-retina/brain transport of [^{3}H]verapamil, the test solutions were injected into the rat common carotid artery of rats anesthetized with pentobarbital. The injected solution was 200 μL Ringer-HEPES buffer containing [^{3}H]verapamil (3 μCi, 188 nM) and a diffusible internal reference, [^{14}C]*n*-butanol (0.5 μCi), with or without cationic compounds. The radioactivity measurements of [^{3}H]verapamil and [^{14}C]*n*-butanol were performed using a liquid scintillation counter (LSC-7400, Aloka, Tokyo, Japan).

The obtained data were analyzed as described in our previous reports (8,16,24–29). In the integration plot analysis, the apparent tissue-to-plasma concentration ratio, over the time-period of the experiment (t), was defined as $V_d(t)$ and was used as an index of the tissue distribution characteristics of [^{3}H]verapamil. $V_d(t)$ can be calculated as the amount of [^{3}H] per gram tissue divided by that per milliliter plasma, and the apparent influx permeability clearance of [^{3}H]verapamil in tissue ($K_{in,\ tissue}$) was determined by using the following Eq. 1:

$$V_d(t) = K_{in,\ tissue} \times AUC(t)/C_p(t) + V_i \quad (1)$$

where AUC(t) (dpm·min/mL), $C_p(t)$ (dpm/mL), and V_i (mL/g tissue) are the area under the plasma concentration time curve of [^{3}H]verapamil from time 0 to t, the plasma [^{3}H]verapamil concentration at time t, and the rapidly equilibrated distribution volume of [^{3}H]verapamil in the tissue, respectively. In the present study, V_i was thought to be comparable with the vascular tissue volume as described elsewhere (8).

The RUI and BUI values reflect the fractional uptake of [^{3}H]verapamil as a percentage of the fractional uptake of [^{14}C]*n*-butanol in the retina and brain, respectively. In the present study, they were used as an index of the distribution characteristics of [^{3}H]verapamil into organs, and can be described by the following Eq. 2;

$$\text{RUI or BUI} = ([^3\text{H}]/[^{14}\text{C}]\ (\text{dpm in the retina or brain}))/([^3\text{H}]/[^{14}\text{C}]\ (\text{dpm in the injectate solution})) \times 100 \quad (2)$$

Cell Culture and Uptake Study

TR-iBRB2 cells (passage number 23-35), a conditionally immortalized rat retinal capillary endothelial cell line, were cultured in Dulbecco's modified Eagle's medium (Nissui Pharmaceuticals, Tokyo, Japan) with 10% fetal bovine serum, 20 mM $NaHCO_3$, and antibiotics, as described previously (5). The optimal growth temperature for TR-iBRB2 cells was set at 33°C because of the expression of temperature-sensitive large T-antigen in TR-iBRB2 cells (24,25). Prior to the uptake study, cells were rinsed with extracellular fluid (ECF)-buffer (122 mM NaCl, 25 mM $NaHCO_3$, 3 mM KCl, 1.4 mM $CaCl_2$, 1.2 mM $MgSO_4$, 0.4 mM K_2HPO_4, 10 mM D-glucose and 10 mM HEPES (pH 7.4)), and the uptake studies were performed at 37°C as described elsewhere (5,24,25). In the present study, the assay buffers were 200 μL of ECF-buffer containing 0.1 μCi [^{3}H]verapamil (6.25 nM) or [^{3}H]pyrilamine (25 nM) at 37°C with or without inhibitors. In the analysis of Na^+-dependent transport, Na^+-free ECF-buffer was prepared by replacement with equimolar LiCl and $KHCO_3$. The radioactivity measurements of [^{3}H]verapamil and [^{3}H]pyrilamine were performed using a liquid scintillation counter (LSC-7400, Aloka), and the cellular protein content was measured by means of a detergent compatible protein assay, according to the manufacturer's instructions (a DC protein assay kit, Bio-Rad, Hercules, CA).

Data analyses of *in vitro* uptake study were performed as described previously (8,16,24–29). In order to express cellular uptake of [^{3}H]verapamil or [^{3}H]pyrilamine, the cell-to-medium ratio was calculated using Eq. 3:

$$\text{Cell/medium ratio} = ([^3\text{H}]\ \text{dpm per cell protein (mg)})/([^3\text{H}]\ \text{dpm per}\ \mu\text{L medium}) \quad (3)$$

To determine kinetic parameters for transport activity, the uptake data of verapamil and pyrilamine were fitted to a one saturable and one nonsaturable process model (Eq. 4) and a two saturable processes model (Eq. 5), respectively.

$$J = J_{max} \times C/(K_m + C) + K_d \times C \quad (4)$$

$$J = J_{max\,1} \times C/(K_{m1} + C) + J_{max\,2} \times C/(K_{m2} + C) \quad (5)$$

In Eq. 4 and Eq. 5, J, C, K_m, J_{max}, and K_d represent the uptake rate, the substrate concentration, the Michaelis constant, the maximal uptake rate and nonsaturable uptake rate, respectively. The nonlinear least-square regression analysis program, MULTI, was used to determine kinetic parameters (30).

The contribution of the saturable process to verapamil uptake was estimated from Eq. 6.

$$\textit{Contribution}(\%) = 100 \times (J_{max}/K_m)/[(J_{max}/K_m) + K_d] \quad (6)$$

Statistical Analysis

Statistical analyses were carried out using a one way analysis of variance (ANOVA) followed by the modified Fisher's least-significant difference method and an unpaired two-tailed Student's *t*-test for several and two groups, respectively. Unless otherwise indicated, all data represent means ± S.E.M. except for kinetic parameters. The data for the kinetic parameters represent means ± S.D.

RESULTS

Blood-to-Retina Transport of Verapamil Across the BRB

The *in vivo* blood-to-retina transport of verapamil across the BRB was evaluated to allow comparison with the blood-to-brain transport across the blood-brain barrier (BBB) using integration plot analysis after intravenous administration of [^{3}H]verapamil to rats (Fig. 1). By means of Eq. 1, the $K_{in,\,retina}$ of [^{3}H]verapamil was determined from the slope representing the apparent influx permeability clearance across the BRB and found to be 614 ± 40 μL/(min·g retina) (Fig. 1a). This is a much higher value than that previously determined for [^{3}H]D-mannitol (0.626 μL/(min·g retina)) (7). The $K_{in,\,brain}$ of [^{3}H]verapamil was 131 ± 32 μL/(min·g brain) (Fig. 1b) which is 4.7-fold lower than that determined for the retina.

In Table I, the greater influx transport of verapamil across the BRB compared with BBB was also supported by the estimated RUI (507%) of [^{3}H]verapamil which was

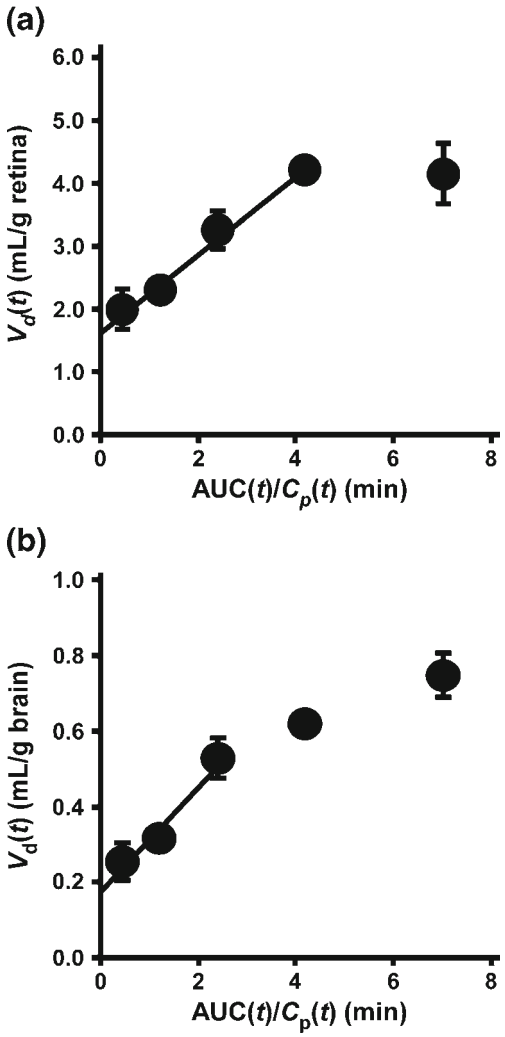

Fig. 1 The initial uptake of [^{3}H]verapamil by the retina (**a**) and brain (**b**) in rats. In the integration plot analysis, [^{3}H]verapamil (3 μCi/rat) was injected into the femoral vein. Each point represents the mean ± S.E.M (n=3–4).

much higher than the BUI (12.1%). Verapamil and quinidine, at a concentration of 3 mM and 10 mM, slightly increased the RUI of [^{3}H]verapamil to 133% and 127% compared with the control, respectively, while the BUI was markedly increased to 799% and 822%, respectively. Pyrilamine, at a concentration of 3 mM, had no significant effect on the RUI, whereas the BUI was increased to 289%. In addition, pyrilamine, at a concentration of 40 mM, significantly reduced the RUI to 72.9% but not for the BUI, and choline at 40 mM had no significant effect on either. These *in vivo* results clearly show the carrier-mediated efflux and influx transport of verapamil across the BRB.

Uptake of [^{3}H]Verapamil by TR-iBRB2 Cells

To investigate the mechanism of verapamil transport across the BRB, an uptake study with TR-iBRB2 cells was performed. TR-iBRB2 cells showed a time-dependent increase in [^{3}H]verapamil uptake for at least 5 min, with an initial uptake rate of 56.9±4.1 μL/(min·mg protein) (Fig. 2a). The effects of Na^+-free buffer and temperature on [^{3}H]verapamil uptake were investigated, and a temperature of 4°C significantly reduced [^{3}H]verapamil uptake by 57% whereas Na^+-free conditions produced no change in [^{3}H]verapamil uptake (Fig. 2a). In addition, no significant effect on [^{3}H]verapamil uptake was exhibited at pH 6.4, and 8.4 (Fig. 2b). The pretreatment of TR-iBRB2 cells with NH_4Cl produced no significant alteration in the [^{3}H]verapamil uptake (data not shown), suggesting that the [^{3}H]verapamil uptake is not affected by intracellular acidification.

Figure 3a shows that the [^{3}H]verapamil uptake by TR-iBRB2 cells took place in a concentration-dependent manner with a K_m of 61.9±3.9 μM, a J_{max} of 3.31±0.21 nmol/(min·mg protein) and a K_d of 5.93±0.95 μL/(min·mg protein). Under the experimental conditions used in the present study, the estimated contribution of the saturable process to verapamil transport was 90%, suggesting that an Na^+-independent carrier-mediated transport system made a major contribution to the verapamil uptake by TR-iBRB2 cells.

Inhibition Study of [^{3}H]Verapamil Uptake with Cationic Compounds

The effect of a number of compounds on the [^{3}H]verapamil uptake by TR-iBRB2 cells is summarized in Table II. Verapamil, desipramine, imipramine, quinidine, memantine, pyrilamine, mecamylamine and amantadine, at concentrations of 500 μM, caused marked inhibition by more than 54%. In addition, β-blockers, such as propranolol, nipradilol and timolol, strongly inhibited [^{3}H]verapamil uptake by more than 55%, and α-agonists, such as clonidine and brimonidine, caused moderate inhibition by more than 35%. Moreover, L-carnitine, a substrates of OCTN2 (Slc22a5), at a concentration of 500 μM, produced a slight inhibition of 23%, whereas similar concentrations of cimetidine, choline, decynium-22, 1-methyl-4-phenylpyridinium (MPP^+), tetraethylammonium (TEA), acetazolamide, serotonin and *p*-aminohyppuric acid (PAH) had no significant effect.

In Fig. 3b, the inhibitory effect of a cationic compound on [^{3}H]verapamil uptake is shown kinetically. Pyrilamine, at a concentration of 200 μM, inhibited verapamil uptake, and the saturable process of [^{3}H]verapamil uptake seems to be inhibited competitively by pyrilamine.

Uptake of [^{3}H]Pyrilamine by TR-iBRB2 Cells

The pharmacological importance of a putative pyrilamine transporter at the BBB has been proposed (32,33), and it was thought to contribute to verapamil transport across the inner BRB. To investigate the characteristics of pyrilamine

Table I The RUI and BUI Values of [^{3}H]Verapamil in Rats

Inhibitor	RUI (%)	% of control	BUI (%)	% of control
Control	507 ± 23	100 ± 5	12.1 ± 1.0	100 ± 8
3 mM Verapamil	676 ± 20*	133 ± 4	96.8 ± 3.9*	799 ± 32
10 mM Quinidine	644 ± 34*	127 ± 7	99.5 ± 7.8*	822 ± 65
3 mM Pyrilamine	506 ± 47	99.9 ± 9.3	35.0 ± 1.8*	289 ± 15
40 mM Pyrilamine	370 ± 46*	72.9 ± 9.0	19.2 ± 1.1	158 ± 9
40 mM Choline	566 ± 70	112 ± 14	14.4 ± 2.9	119 ± 24

[^{3}H]Verapamil (3 μCi/rat) and [^{14}C]*n*-butanol (0.5 μCi/rat) were injected into the common carotid artery in the absence (control) or presence of inhibitors. Forty mM pyrilamine was used by according to the previous report on the BUI study of [^{3}H]naloxone (31). Ten mM quinidine and 3 mM verapamil were set because of its limitation of solubility, and 3 mM pyrilamine was set to compare the effect of pyrilamine to that of verapamil. Forty mM choline was a negative control since the highest concentration of inhibitors was 40 mM. Each value represents means ± S.E.M. (n=3–16). *$p < 0.01$, significantly different from the control

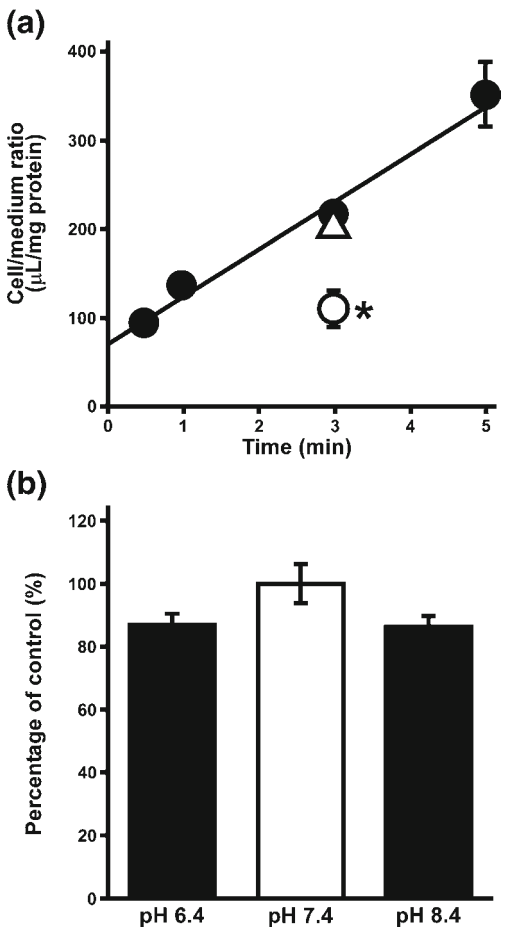

Fig. 2 Uptake of [^{3}H]verapamil by TR-iBRB2 cells. (**a**) The time-course (closed circle) of [^{3}H]verapamil uptake (6.25 nM) was examined at 37°C. Temperature- (4°C; open circle) and Na^+- (open triangle) dependence of the [^{3}H]verapamil uptake was examined in ECF-buffer with (control; closed circle) or without Na^+. (**b**) The pH-dependence (pH 6.4 and 8.4) was also examined. Except for the time-course and temperature-dependent studies, the uptake was performed at 37°C for 3 min. The cell uptake of [^{3}H]verapamil was expressed using the cell/medium ratio, and each point and column represents the mean ± S.E.M (n=3–4). *$p < 0.01$, significantly different from the control.

transport at the inner BRB, the [^{3}H]pyrilamine uptake by TR-iBRB2 cells was investigated. TR-iBRB2 cells exhibited a time-dependent increase in [^{3}H]pyrilamine uptake for at least 30 sec, with an initial uptake rate of 112 ± 9 μL/(min·mg protein) (Fig. 4a). [^{3}H]Pyrilamine uptake exhibited a significant reduction (by 49%) at 4°C (Fig. 4b) and, at pH 8.4, there was a significantly higher [^{3}H]pyrilamine uptake (by 27%) compared with the control (pH 7.4) (Fig. 4c). The [^{3}H]pyrilamine uptake was shown to be concentration-dependent, with a K_{m1} of 20.2 ± 4.4 μM, a J_{max1} of 0.837 ± 0.179 nmol/(min·mg protein), a K_{m2} of 252 ± 6 μM and a J_{max2} of 22.3 ± 0.8 nmol/(min·mg protein) (Fig. 5a).

To clarify the transport properties of the [^{3}H]pyrilamine uptake in TR-iBRB2 cells, the inhibitory effects of several compounds were examined (Table II). Verapamil, at a concentration of 500 μM, strongly inhibited [^{3}H]pyrilamine uptake by 79%. In addition, desipramine, imipramine, propranolol, memantine, quinidine, nipradilol, amantadine, clonidine and timolol, at a concentration of 500 μM, caused marked inhibition by more than 51% while no inhibitory effects on [^{3}H]pyrilamine uptake were observed in the presence of TEA, serotonin, L-carnitine and choline.

In Fig. 5b, the inhibitory effect of verapamil on [^{3}H]pyrilamine uptake was kinetically studied. Verapamil, at a concentration of 100 μM, inhibited pyrilamine uptake, and no intersection of the two lines of pyrilamine uptake on the abscissa in the presence or absence of 100 μM verapamil was observed, indicating no competitive inhibition of saturable pyrilamine transport by verapamil.

DISCUSSION

Verapamil is known as a cationic substrate of P-gp, which is expressed in various tissues such as the BBB, and is involved in the efflux transport of drugs (17–19). At the BRB, P-gp is expressed in retinal capillary endothelial cells (inner BRB) and RPE cells (outer BRB) to remove xenobiotics to the

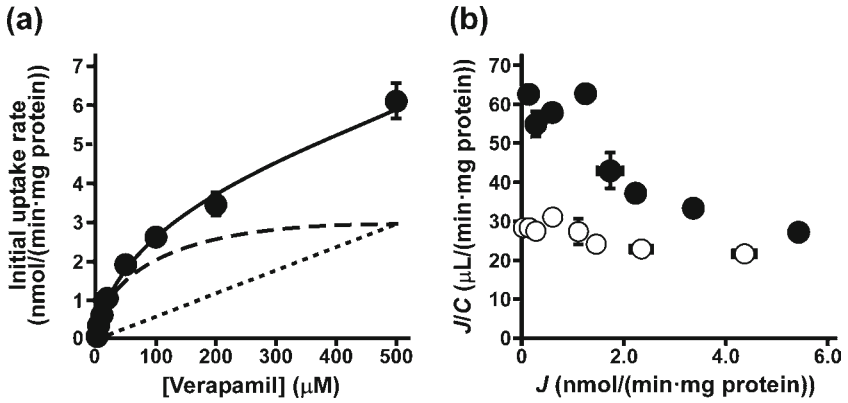

Fig. 3 Concentration-dependent uptake of [^{3}H]verapamil. The uptake of [^{3}H]verapamil by TR-iBRB2 cells was examined at 37°C for 3 min. (**a**) Data obtained over the concentration range studied (1–500 μM), were analyzed by Michaelis-Menten kinetics. The dotted, dashed and solid lines represent the best fit to nonsaturable transport, saturable transport and the overall transport data, respectively. (**b**) [^{3}H]verapamil uptake (at a concentration of 2–200 μM) with (open circle) or without (closed circle) 200 μM pyrilamine was performed, and an Eadie-Scatchard plot was used in the data analysis. Each point represents the mean ± S.E.M. (n=3).

circulating blood, and the contribution of P-gp at the inner BRB is reported to be lower than that of the BBB (12,13). Our previous reports have suggested the possible involvement of carrier-mediated influx process(es) in verapamil transport from the circulating blood to the retina across the BRB, and these influx process(es) could be useful for systemic drug delivery to the retina, since drugs for ocular diseases include several cationic ones, although the detailed transport mechanism is unclear (16,23). In the present study, *in vivo* and *in vitro* analyses were performed to investigate the functional properties of verapamil influx transport across the inner BRB, and our results suggest the involvement of a novel organic cation transporter at the inner BRB.

Integration plot analysis showed that the transport of [^{3}H]verapamil from the blood to the retina across the BRB had a far higher $K_{in,\ retina}$ (614 μL/(min·g retina); Fig. 1a) than that of D-mannitol, a non-permeable paracellular marker (7), which suggested the permeation of verapamil into retina from the circulating blood. Combined with this result and our previous report that verapamil exhibits a 5.3-fold higher RUI value than that estimated from its lipophilicity (16), the involvement of an influx transport system is suggested in verapamil transport across the BRB. The $K_{in,\ retina}$ value is 4.7-fold higher than the $K_{in,\ brain}$ (131 μL/(min·g brain); Fig. 1b), and tissue uptake index analysis also showed a higher RUI (507%) than BUI (12.1%) for [^{3}H]verapamil (Table I), which implies the influx transport of verapamil at the BRB works more greatly than that of the BBB. In the inhibition study of the tissue uptake index, 3 mM verapamil and 10 mM quinidine had a significantly higher effect, with approximately 1.3- and 8.0-fold greater, RUI and BUI values of [^{3}H]verapamil than controls while 40 mM choline had no significant effects (Table I). These results support the P-gp-mediated efflux of verapamil across the BRB since verapamil and quinidine

Table II Effect of Compounds on [^{3}H]Verapamil and [^{3}H]Pyrilamine Uptake by TR-iBRB2 Cells

Compound	Relative Uptake (% of control)	
	[^{3}H]Verapamil	[^{3}H]Pyrilamine
Control	100 ± 3	100 ± 2
Desipramine	7.20 ± 0.26*	2.13 ± 0.10*
Propranolol	9.45 ± 0.21*	16.7 ± 1.1*
Imipramine	9.65 ± 0.09*	2.54 ± 0.02*
Quinidine	17.2 ± 0.5*	24.9 ± 0.9*
Verapamil	19.6 ± 1.4*	21.2 ± 0.2*
Memantine	27.9 ± 2.9*	24.1 ± 1.3*
Nipradilol	31.1 ± 1.2*	13.7 ± 0.23*
Pyrilamine	31.3 ± 1.2*	42.2 ± 0.8*
Mecamylamine	41.8 ± 1.8*	N.D.
Timolol	44.5 ± 4.5*	48.2 ± 0.4*
Amantadine	45.6 ± 1.3*	43.0 ± 1.1*
Clonidine	63.3 ± 3.5*	48.1 ± 1.2*
Brimonidine	65.0 ± 3.6*	N.D.
L-Carnitine	76.9 ± 12.8*	129 ± 4
Cimetidine	94.3 ± 3.0	N.D.
Choline	101 ± 14	126 ± 2
Decynium-22	103 ± 6	N.D.
MPP^+	105 ± 9	N.D.
TEA	119 ± 5	149 ± 1
Acetazolamide	121 ± 17	N.D.
Serotonin	131 ± 11	119 ± 2
PAH	133 ± 4	N.D.

[^{3}H]Verapamil uptake by TR-iBRB2 cells was performed in the absence (control) or presence of 500 μM compounds at 37°C for 3 min. Similarly, [^{3}H]Pyrilamine uptake by TR-iBRB2 cells was performed at 37°C for 30 sec. Each value represents means ± S.E.M. (n=3–16). *p < 0.01, significantly different from the control. MPP^+, 1-methyl-4-phenylpyridinium; TEA, tetraethylammonium; PAH, *p*-aminohippuric acid., N.D.; not determined

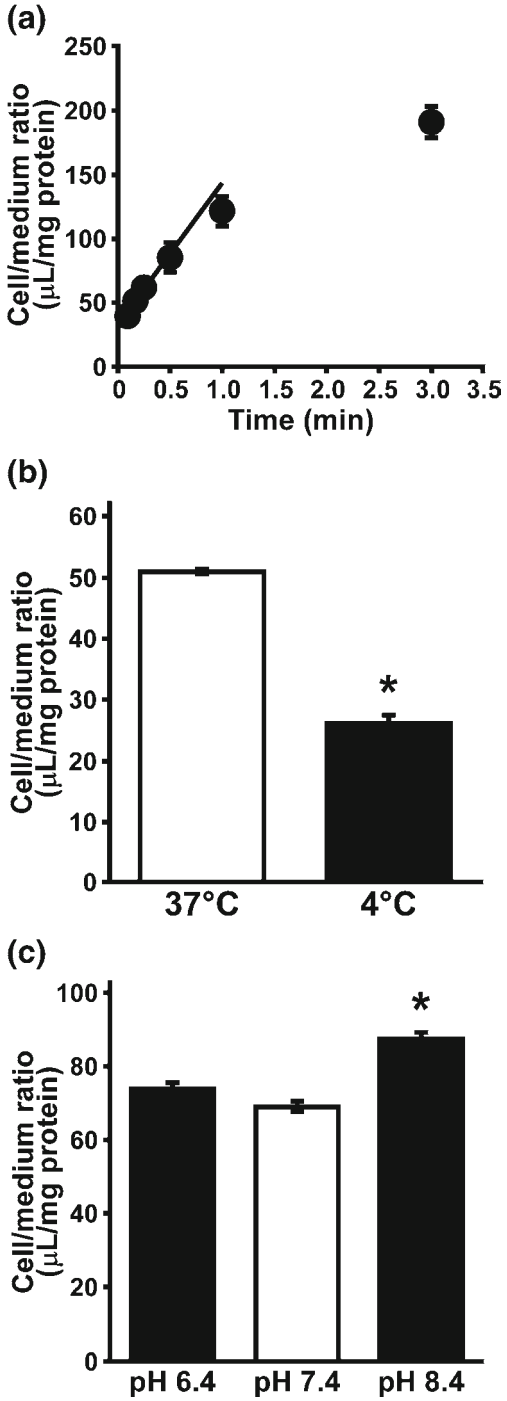

Fig. 4 Uptake of [^{3}H]pyrilamine by TR-iBRB2 cells. (**a**) The time-course of [^{3}H]pyrilamine uptake (25 nM) was examined at 37°C. (**b**) The temperature-dependence was examined at 37°C or 4°C for 10 sec. (**c**) The pH-dependence (pH 6.4 and 8.4) was examined at 37°C for 30 sec. Each point and column represents the mean ± S.E.M (n=3–5). *$p < 0.01$, significantly different from the control.

are a substrate and an inhibitor of P-gp, respectively, and the lower increases in RUI compared with BUI support the lower contribution of P-gp at the BRB compared with the BBB (12,16). Choline is known to be an endogenous cation, and the results in the presence of choline suggest that choline transport system(s) make only a minor contribution to the transport of verapamil at the BRB and BBB (Table I) (34–36). On the other hand, in the presence of pyrilamine, the RUI and BUI values of [^{3}H]verapamil were affected differently (Table I). In particular, pyrilamine, at a concentration of 40 mM, significantly reduced the RUI value during the 1.6-fold increase in the BUI value, confirming the pyrilamine-sensitive carrier-mediated influx transport of verapamil at the BRB.

The *in vivo* analyses suggested carrier-mediated influx transport of verapamil at the inner BRB (Fig. 1 and Table I). However, little is known about organic cation transport systems at the inner BRB while putative organic cation transporters have been reported at the outer BRB (20,37). Therefore, the uptake of [^{3}H]verapamil was examined using an *in vitro* inner BRB model, TR-iBRB2 cells. The uptake study suggests that the influx transport of verapamil across the inner BRB took place in a time- and temperature-dependent manner and was also Na^+- and pH-independent (Fig. 2a and b). The concentration-dependence of the verapamil influx transport was also suggested with a K_d of 5.93 μL/(min·mg protein), a J_{max} of 3.31 nmol/(min·mg protein) and a K_m of 61.9 μM, confirming the major contribution of the saturable process (Fig. 3a). These results clearly support the involvement of a carrier-mediated transport system in the influx transport of verapamil across the inner BRB.

In the inhibition study in TR-iBRB2 cells, verapamil and quinidine inhibited the [^{3}H]verapamil uptake while they exhibited higher RUI and BUI values than that of the controls. Considering this discrepancy, it would appear that the amount of P-gp expressed in TR-iBRB2 cells is low compared with *in vivo* condition. The results of inhibition study suggest the involvement of a novel organic cation transporter in the influx transport of verapamil across the inner BRB since [^{3}H]verapamil uptake was significantly inhibited by cationic compounds such as imipramine, quinidine, memantine, pyrilamine, mecamylamine, timolol, clonidine and amantadine. The specificity for cations is supported by a lack of effect by PAH which is a typical anionic compound, and the competitive-like inhibition shown by pyrilamine (Table II and Fig. 3b). The chemical properties of the compounds used, such as the log *DC* and functional groups, imply that the novel organic cation transporter preferentially recognizes lipophilic compounds with secondary or tertiary amines as its substrates since the most marked inhibition (more than 80%) was exhibited by desipramine, imipramine, propranolol and qunidine. In addition, the inhibition study implies that drugs with anti-angiogenic and neuroprotectant properties for ocular diseases can be the substrates of the novel organic cation transporter because of the significant inhibition produced

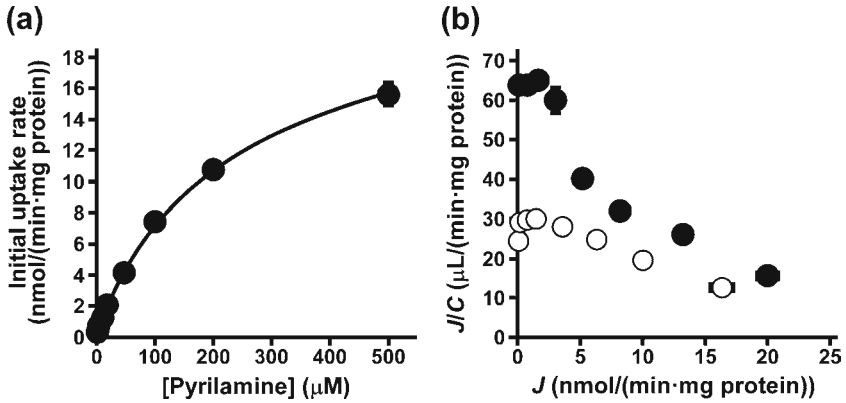

Fig. 5 Concentration-dependent uptake of [^{3}H]pyrilamine. (**a**) The uptake of [^{3}H]pyrilamine (25 nM) by TR-iBRB2 cells was studied at 37°C for 30 sec. Data, obtained over the concentration range studied (2–500 μM), were analyzed by Michaelis-Menten kinetics. (**b**) [^{3}H]Pyrilamine uptake with (open circle) or without (closed circle) 100 μM verapamil was examined, and an Eadie-Scatchard plot was used in the data analysis. Each point represents the mean ± S.E.M (n=3).

by propranolol, desipramine, nipradilol, and brimonidine (Table II). According to previous reports, neuroprotective effects are exhibited by desipramine, nipradilol, and brimonidine, a tricyclic antidepressant, a β-adrenergic antagonist and an α_2-adrenergic agonist, respectively, and propranolol, a β-adrenergic antagonist, is protective against retinal angiogenesis (38–41). The novel organic cation transporter at the inner BRB is suggested to be different from well-characterized organic cation transporters, such as OCT1 (Slc22a1) (42), OCT2 (Slc22a2) (43,44), OCT3 (Slc22a3) (45), OCTN1 (Slc22a4) (46,47), OCTN2 (Slc22a5) (48,49), MATE1 (Slc47a1) (50,51) and PMAT (Slc29a4/ENT4) (52), since their substrates and inhibitors, such as TEA, MPP^+, decynium-22, choline, and cimetidine, had no significant effects on the [^{3}H] verapamil uptake by TR-iBRB2 cells (Table II). Although the significant inhibition by L-carnitine implies the possible involvement of OCTN2, it is reasonable to suppose that OCTN2 is not identical to the novel organic cation transporter at the inner BRB because its other substrates and inhibitors, such as TEA, MPP^+ and cimetidine, had no effect (Table II) (48,49). Therefore, the identity of the molecule responsible for verapamil transport at the inner BRB remains unclear (Supplementary Material Fig. S1).

Regarding reported putative organic cation transporters at the tissue barriers, a putative verapamil transporter and a putative pyrilamine transporter have suggested at the outer BRB and BBB, respectively (20,32,33). The verapamil transporter at the outer BRB is reported to act in a pH-dependent manner (20), indicating that it has a different pH-sensitivity from the verapamil transport across the inner BRB (Fig. 2b). On the other hand, the contribution of the pyrilamine transporter was examined in TR-iBRB2 cells since pyrilamine exhibited an inhibitory effect on the [^{3}H] verapamil uptake (Table II and Fig. 3b). The results of the [^{3}H]pyrilamine uptake study suggested that the pyrilamine transport across the inner BRB takes place in a temperature-, pH- and concentration-dependent manner (Fig. 4), and involves high-affinity (K_{m1}=20.2 μM) and low-affinity (K_{m2}=252 μM) processes (Fig. 5a), implying a similar pyrilamine affinity between the high-affinity process and the putative pyrilamine transporter at the BBB (32). In the inhibition study, L-carnitine exhibited no significant effect on [^{3}H]pyrilamine uptake by TR-iBRB2 cells, of which sensitivity to L-carnitine is different from that of [^{3}H] verapamil uptake, whereas significant inhibitory effects were observed in the presence of desipramine, propranolol, imipramine, quinidine, verapamil, memantine, nipradilol, pyrilamine, timolol, amantadine and clonidine. The different pH-sensitivity of verapamil and pyrilamine uptake by TR-iBRB2 cells indicates that their molecules responsible are not identical, and this is also supported by their different sensitivity to L-carnitine (Table II) (Supplementary Material Fig. S1). The kinetic analysis indicates that verapamil has no competitive effect on the pyrilamine uptake although verapamil uptake exhibited a competitive-like inhibition (Fig. 3b and Fig. 5b), supporting the belief that the verapamil transport system differs from that of pyrilamine in spite of its sensitivity to pyrilamine.

In conclusion, our investigations suggest that a carrier-mediated transport system is involved in the verapamil transport from the circulating blood to the retina. Its transport properties are clearly different from those of well-characterized organic cation transporter molecules, suggesting that a novel organic cation transporter is involved in the influx transport of verapamil at the inner BRB. Furthermore, the inhibition study revealed the possible role of this novel organic cation transporter in the distribution of cationic drugs, including anti-angiogenic compounds and neuroprotectants, to the neural retina. The present findings provide helpful information to increase our understanding of drug transport at the BRB with the future possibility of designing suitable methods for systemic drug delivery to the retina.

ACKNOWLEDGMENTS AND DISCLOSURES

We would like to thank Kowa Co., Ltd. for providing nipradilol. The present study was supported, in part, by a Grant-in-Aid for Scientific Research from the Japan Society for the Promotion of Science (JSPS), Health and Welfare Department of Toyama Prefectural Government (Toyama, Japan), and Mochida Memorial Foundation (Tokyo, Japan).

Y. Kubo and Y. Kusagawa contributed equally to this work.

REFERENCES

1. Cunha-Vaz JG. The blood-retinal barriers system. Basic concepts and clinical evaluation. Exp Eye Res. 2004;78:715–21.
2. Stewart PA, Tuor UI. Blood-eye barriers in the rat: correlation of ultrastructure with function. J Comp Neurol. 1994;340:566–76.
3. Hosoya K, Tomi M, Tachikawa M. Strategies for therapy of retinal diseases using systemic drug delivery: relevance of transporters at the blood-retinal barrier. Expert Opin Drug Deliv. 2011;8:1571–87.
4. Takata K, Kasahara T, Kasahara M, Ezaki O, Hirano H. Ultracytochemical localization of the erythrocyte/HepG2-type glucose transporter (GLUT1) in cells of the blood-retinal barrier in the rat. Invest Ophthalmol Vis Sci. 1992;33:377–83.
5. Hosoya K, Kondo T, Tomi M, Takanaga H, Ohtsuki S, Terasaki T. MCT1-mediated transport of L-lactic acid at the inner blood-retinal barrier: a possible route for delivery of monocarboxylic acid drugs to the retina. Pharm Res. 2001;18:1669–76.
6. Tomi M, Mori M, Tachikawa M, Katayama K, Terasaki T, Hosoya K. L-type amino acid transporter 1-mediated L-leucine transport at the inner blood-retinal barrier. Invest Ophthalmol Vis Sci. 2005;46:2522–30.
7. Tachikawa M, Takeda Y, Tomi M, Hosoya K. Involvement of OCTN2 in the transport of acetyl-L-carnitine across the inner blood-retinal barrier. Invest Ophthalmol Vis Sci. 2010;51:430–6.
8. Ohkura Y, Akanuma S, Tachikawa M, Hosoya K. Blood-to-retina transport of biotin *via* Na+-dependent multivitamin transporter (SMVT) at the inner blood-retinal barrier. Exp Eye Res. 2010;91:387–92.
9. Hosoya K, Makihara A, Tsujikawa Y, Yoneyama D, Mori S, Terasaki T, *et al.* Roles of inner blood-retinal barrier organic anion transporter 3 in the vitreous/retina-to-blood efflux transport of *p*-aminohippuric acid, benzylpenicillin, and 6-mercaptopurine. J Pharmacol Exp Ther. 2009;329:87–93.
10. Tomi M, Hosoya K. Application of magnetically isolated rat retinal vascular endothelial cells for the determination of transporter gene expression levels at the inner blood-retinal barrier. J Neurochem. 2004;91:1244–8.
11. Tagami M, Kusuhara S, Honda S, Tsukahara Y, Negi A. Expression of ATP-binding cassette transporters at the inner blood-retinal barrier in a neonatal mouse model of oxygen-induced retinopathy. Brain Res. 2009;1283:186–93.
12. Shen J, Cross ST, Tang-Liu DD, Welty DF. Evaluation of an immortalized retinal endothelial cell line as an *in vitro* model for drug transport studies across the blood-retinal barrier. Pharm Res. 2003;20:1357–63.
13. Kennedy BG, Mangini NJ. P-glycoprotein expression in human retinal pigment epithelium. Mol Vis. 2002;8:422–30.
14. Kadam RS, Kompella UB. Influence of lipophilicity on drug partitioning into sclera, choroid-retinal pigment epithelium, retina, trabecular meshwork, and optic nerve. J Pharmacol Exp Ther. 2010;332:1107–20.
15. Toda R, Kawazu K, Oyabu M, Miyazaki T, Kiuchi Y. Comparison of drug permeabilities across the blood-retinal barrier, blood-aqueous humor barrier, and blood-brain barrier. J Pharm Sci. 2011;100:3904–11.
16. Hosoya K, Yamamoto A, Akanuma S, Tachikawa M. Lipophilicity and transporter influence on blood-retinal barrier permeability: a comparison with blood-brain barrier permeability. Pharm Res. 2010;27:2715–24.
17. Bankstahl JP, Kuntner C, Abrahim A, Karch R, Stanek J, Wanek T, *et al.* Tariquidar-induced P-glycoprotein inhibition at the rat blood-brain barrier studied with (R)-^{11}C-verapamil and PET. J Nucl Med. 2008;49:1328–35.
18. Tsuji A, Terasaki T, Takabatake Y, Tenda Y, Tamai I, Yamashima T, *et al.* P-glycoprotein as the drug efflux pump in primary cultured bovine brain capillary endothelial cells. Life Sci. 1992;51:1427–37.
19. Schinkel AH, Wagenaar E, van Deemter L, Mol CA, Borst P. Absence of the mdr1a P-Glycoprotein in mice affects tissue distribution and pharmacokinetics of dexamethasone, digoxin, and cyclosporin A. J Clin Invest. 1995;96:1698–705.
20. Han YH, Sweet DH, Hu DN, Pritchard JB. Characterization of a novel cationic drug transporter in human retinal pigment epithelial cells. J Pharmacol Exp Ther. 2001;296:450–7.
21. Elliott WJ, Ram CV. Calcium channel blockers. J Clin Hypertens. 2011;13:687–9.
22. Araie M, Mayama C. Use of calcium channel blockers for glaucoma. Prog Retin Eye Res. 2011;30:54–71.
23. Kubo Y, Fukui E, Akanuma S, Tachikawa M, Hosoya K. Application of membrane permeability evaluated in *in vitro* analyses to estimate blood-retinal barrier permeability. J Pharm Sci. 2012;101:2596–605.
24. Hosoya K, Tomi M, Ohtsuki S, Takanaga H, Ueda M, Yanai N, *et al.* Conditionally immortalized retinal capillary endothelial cell lines (TR-iBRB) expressing differentiated endothelial cell functions derived from a transgenic rat. Exp Eye Res. 2001;72:163–72.
25. Hosoya K, Tomi M. Advances in the cell biology of transport *via* the inner blood-retinal barrier: establishment of cell lines and transport functions. Biol Pharm Bull. 2005;28:1–8.
26. Hosoya K, Minamizono A, Katayama K, Terasaki T, Tomi M. Vitamin C transport in oxidized form across the rat blood-retinal barrier. Invest Ophthalmol Vis Sci. 2004;45:1232–39.
27. Ohtsuki S, Tachikawa M, Takanaga H, Shimizu H, Watanabe M, Hosoya K, *et al.* The blood-brain barrier creatine transporter is a major pathway for supplying creatine to the brain. J Cereb Blood Flow Metab. 2002;22:1327–35.
28. Alm A, Törnquist P. The uptake index method applied to studies on the blood-retinal barrier. I. A methodological study. Acta Physiol Scand. 1981;113:73–9.
29. Pardridge WM, Fierer G. Blood-brain barrier transport of butanol and water relative to N-isopropyl-p-iodoamphetamine as the internal reference. J Cereb Blood Flow Metab. 1985;5:275–81.
30. Yamaoka K, Tanigawara Y, Nakagawa T, Uno T. A pharmacokinetic analysis program (MULTI) for microcomputer. J Pharmacobiodyn. 1981;4:879–85.
31. Suzuki T, Ohmuro A, Miyata M, Furuishi T, Hidaka S, Kugawa F, *et al.* Involvement of an influx transporter in the blood-brain barrier transport of naloxone. Biopharm Drug Dispos. 2010;31:243–52.
32. Yamazaki M, Terasaki T, Yoshioka K, Nagata O, Kato H, Ito Y, *et al.* Carrier-mediated transport of H_1-antagonist at the blood-brain barrier: a common transport system of H_1-antagonists and lipophilic basic drugs. Pharm Res. 1994;11:1516–8.
33. Okura T, Hattori A, Takano Y, Sato T, Hammarlund-Udenaes M, Terasaki T, *et al.* Involvement of the pyrilamine transporter, a

putative organic cation transporter, in blood-brain barrier transport of oxycodone. Drug Metab Dispos. 2008;36:2005–13.
34. Murakami H, Sawada N, Koyabu N, Ohtani H, Sawada Y. Characteristics of choline transport across the blood-brain barrier in mice: correlation with *in vitro* data. Pharm Res. 2000;17:1526–30.
35. Karlsson C, Mäepea O, Alm A. Choline transport through the blood-retinal and the blood-brain barrier *in vivo*. Acta Ophthalmol (Copenh). 1984;62:763–6.
36. Tomi M, Arai K, Tachikawa M, Hosoya K. Na^+-independent choline transport in rat retinal capillary endothelial cells. Neurochem Res. 2007;32:1833–42.
37. Zhang N, Kannan R, Okamoto CT, Ryan SJ, Lee VH, Hinton DR. Characterization of brimonidine transport in retinal pigment epithelium. Invest Ophthalmol Vis Sci. 2006;47:287–94.
38. Mizuno K, Koide T, Yoshimura M, Araie M. Neuroprotective effect and intraocular penetration of nipradilol, a beta-blocker with nitric oxide donative action. Invest Ophthalmol Vis Sci. 2001;42:688–94.
39. Arthur S, Cantor LB. Update on the role of alpha-agonists in glaucoma management. Exp Eye Res. 2011;93:271–83.
40. Lauterbach EC, Victoroff J, Coburn KL, Shillcutt SD, Doonan SM, Mendez MF. Psychopharmacological neuroprotection in neurodegenerative disease: assessing the preclinical data. J Neuropsychiatry Clin Neurosci. 2010;22(1):8–18.
41. Ristori C, Filippi L, Dal Monte M, Martini D, Cammalleri M, Fortunato P, *et al.* Role of the adrenergic system in a mouse model of oxygen-induced retinopathy: antiangiogenic effects of beta-adrenoreceptor blockade. Invest Ophthalmol Vis Sci. 2011;52:155–70.
42. Gründemann D, Gorboulev V, Gambaryan S, Veyhl M, Koepsell H. Drug excretion mediated by a new prototype of polyspecific transporter. Nature. 1994;372:549–52.
43. Urakami Y, Okuda M, Masuda S, Saito H, Inui K. Functional characteristics and membrane localization of rat multispecific organic cation transporters, OCT1 and OCT2, mediating tubular secretion of cationic drugs. J Pharmacol Exp Ther. 1998;287:800–5.
44. Gründemann D, Babin-Ebell J, Martel F, Ording N, Schmidt A, Schömig E. Primary structure and functional expression of the apical organic cation transporter from kidney epithelial LLC-PK1 cells. J Biol Chem. 1997;272:10408–13.
45. Kekuda R, Prasad PD, Wu X, Wang H, Fei YJ, Leibach FH, *et al.* Cloning and functional characterization of a potential-sensitive, polyspecific organic cation transporter (OCT3) most abundantly expressed in placenta. J Biol Chem. 1998;273:15971–9.
46. Wu X, George RL, Huang W, Wang H, Conway SJ, Leibach FH, *et al.* Structural and functional characteristics and tissue distribution pattern of rat OCTN1, an organic cation transporter, cloned from placenta. Biochim Biophys Acta. 2000;1466:315–27.
47. Yabuuchi H, Tamai I, Nezu J, Sakamoto K, Oku A, Shimane M, *et al.* Novel membrane transporter OCTN1 mediates multispecific, bidirectional, and pH-dependent transport of organic cations. J Pharmacol Exp Ther. 1999;289:768–73.
48. Wu X, Huang W, Prasad PD, Seth P, Rajan DP, Leibach FH, *et al.* Functional characteristics and tissue distribution pattern of organic cation transporter 2 (OCTN2), an organic cation/carnitine transporter. J Pharmacol Exp Ther. 1999;290:1482–92.
49. Ohashi R, Tamai I, Yabuuchi H, Nezu JI, Oku A, Sai Y, *et al.* Na^+-dependent carnitine transport by organic cation transporter (OCTN2): its pharmacological and toxicological relevance. J Pharmacol Exp Ther. 1999;291:778–84.
50. Otsuka M, Matsumoto T, Morimoto R, Arioka S, Omote H, Moriyama Y. A human transporter protein that mediates the final excretion step for toxic organic cations. Proc Natl Acad Sci U S A. 2005;102:17923–8.
51. Ohta KY, Inoue K, Hayashi Y, Yuasa H. Molecular identification and functional characterization of rat multidrug and toxin extrusion type transporter 1 as an organic cation/H^+ antiporter in the kidney. Drug Metab Dispos. 2006;34:1868–74.
52. Engel K, Wang J. Interaction of organic cations with a newly identified plasma membrane monoamine transporter. Mol Pharmacol. 2005;68:1397–407.